PR13 Development on Neutron Imaging Application

Y. Saito

Research Reactor Institute, Kyoto University

1. Objectives and Allotted Research Subjects

Neutron imaging provides valuable information which cannot be obtained from an optical or X-ray imaging. The purpose of this project is to develop the imaging method itself and also the experimental environment for expanding the application area of the neutron imaging. The allotted research subjects are as follows:

ARS-1 Measurements of Multiphase Dynamics by Neutron Radiography (Y. Saito *et al.*)
ARS-2 Visualization and Measurement of Flow Behavior in Industrial Equipment (N. Takenaka *et al.*)
ARS-3 Visualization and Measurement of Adsorption/Desorption Process of Ethanol in Activated Carbon Adsorber for Adsorption Heat Pump (N. Asano *et al.*)
ARS-4 Neutron Radiography on Tubular Flow Reactor for Supercritical Hydrothermal Synthesis of Nanoparticles (T. Tsukada *et al.*)
ARS-5 Characteristics of the Void Fraction under Transient Condition (H. Umekawa *et al.*)
ARS-6 Estimation of the Frosting and Defrosting Phenomena by Using Neutron Radiography (R. Matsumoto *et al.*)
ARS-7 Neutron imaging and optics development using simulation of VCAD Systems (Y. Yamagata *et al.*)
ARS-8 Water and Salt Distribution in a Rice Hull Medium under Sodium Chloride Solution Culture (U. Matsushima *et al.*)
ARS-9 Measurement of Water Content in Hardened Cement Paste by Neutron Imaging (T. Numao *et al.*)
ARS-10 In-situ Neutron Radiography Investigation on the Hydraulic Behavior of High Strength Cement Paste under High Temperature (M. Kanematsu *et al.*)
ARS-11 Evaluation of coolant distribution in a flat heat-pipe type heat spreader (K. Mizuta *et al.*)
ARS-12 Visualization of Organic Materials for Development of Industrial Applications (A. Uritani *et al.*)
ARS-13 Visualization of Coolant Flow in a Micro-Structured Wick (Y. Tsuji *et al.*)

2. Main results and the contents of this report

Due to the termination of KUR, no neutron imaging has been performed for fiscal 2016. However, some results have been obtained by analyzing existing experimental results or by performing X-ray imaging as follows:

ARS-2 applied X-ray imaging to two-phase flow across horizontal tube bundles of in-line and staggered. X-ray radiography was employed for the measurement of void fraction distributions. The transmitted X-ray was converted to visible rays using an image intensifier, and the 10-bit gray-scale radiographs were taken using a high-speed camera (MotionPro Y-4 Lite, IDT Inc.) with an array of 1024 × 1024 pixels and with a pixel size of 170 μm. The flame rate was set at 30 fps and 450 radiographs which correspond to 15 s were taken in each condition. The X-ray was generated at 80 kV and 5 mA. From X-ray visualization, two-dimensional void fraction profiles were obtained varying gas- and liquid-superficial velocities. Heat transfer characteristics in two-phase flow across horizontal tubes are clarified also from heat transfer experiments. For bubbly flow condition, heat transfer coefficient between ±90 to ±180° was higher than that in single-phase flow. Void fraction around upstream of the tube was higher than that in the others. Liquid flow agitation by bubbles motion improved the heat transfer around the tube. Under intermittent flow condition, heat transfer coefficient flatten over the tube in comparison to that in single-phase flow. Since the void fraction around the tube was almost uniformly distributed, enhancement of the heat transfer could be obtained by bubbles motion over the entire perimeter of the tube under the condition.

ARS-6 applied X-ray radiography to frosting behavior in cooling heat exchange system. Frost layer was clearly visualized by the X-ray imaging system in the B-4 port of KUR. The X-ray generator was operated at 80kV and 5mA similar to ARS-2. To estimate the frost profile quantitatively, the mass attenuation coefficient of the water and the ice were measured. Experimental results indicate that the mass attenuation coefficient of the ice shows higher value than that of the water. Finaly Abel inversion was applied to the X-ray image to reconstruct the frost density profiles under the circularly symmetric frost formation around the cylindrical surface. In addition, 3-dimensional measurement of the frost deposition was tried by using the newly developed X-ray CT system. On the present step of this research, the 3-D frost density distribution is not success due to the less attenuation by the frost layer on the X-ray CT. In the next stage, the X-ray imaging conditions are modified.

PR13-1 Void Fraction and Heat Transfer Characteristics in Two-Phase Flow across a Horizontal Tube Bundle

H. Murakawa, M. Baba, T. Miyazaki, K. Sugimoto,
H. Asano, N. Takenaka, D. Ito[1] and Y. Saito[1]

Department of Mechanical Engineering, Kobe University
[1]Research Reactor Institute, Kyoto University

INTRODUCTION: Heat exchangers such like shell and tube type are commonly used in process industry, chemical industry, and geothermal power plant. To clarify the two-phase flow structures, many experimental studies have been carried out in a rectangular channel with the tube bundle [1-3]. However, many of these investigation evaluate local void fraction at several measurement positions in the tube bundles, and the measurement of the two-dimensional void fraction distributions in the bundles has not been sufficiently carried out.
In this study, two-dimensional void fractions around a tube were obtained by using X-ray radiography. Local heat transfer coefficients were measured by using an electrode made of platinum wire placed on a tube, and the interaction between the void fraction and heat transfer coefficient distributions were investigated.

EXPERIMENTS: The test section was a vertical duct with a cross-section of 90 × 90 mm^2. Air was injected into the test section through two porous tubes located at the bottom of the test section. Tube arraignment was an in-line tube bundle with 8 rows of three full tubes and two half tubes. The tubes were 90 mm long and the outer diameter, d, was 15 mm. The tubes pitch, p, was 22.5 mm and the pitch-to-diameter ratio, p/d, was 1.5. The experiments were performed at 20–25 ºC under atmospheric pressure condition.
X-ray radiography was employed for the measurement of void fraction distributions. The transmitted X-ray was converted to visible rays using an image intensifier, and the 10-bit gray-scale radiographs were taken using a high-speed camera (MotionPro Y-4 Lite, IDT Inc.) with an array of 1024 × 1024 pixels and with a pixel size of 170 μm. The flame rate was set at 30 fps and 450 radiographs which correspond to 15 sec were taken in each condition. The X-ray was generated at 80 kV and 5 mA.

RESULTS: Results of two-dimensional void fraction distributions are shown in Fig. 1. The superficial liquid velocity, J_L, is 0.2 m/s, and the superficial gas velocity, J_G, is 0.12 and 0.77 m/s. The flow regimes are bubbly and intermittent flows, respectively. The measurement area is around center tube at the 4th row from the inlet of the bundles. Figure 2 shows the heat transfer coefficients around the tube. 0° indicates at the bottom of the tube, and the counterclockwise rotation is defined as positive degree.
Heat transfer coefficient under liquid single-phase flow increases from 0° and takes the maximum values near ± 90°, thereafter takes the minimum values around ± 135°. For bubbly flow condition, heat transfer coefficient between ± 90 to ± 180° was higher than that in single-phase flow. Void fraction around upstream of the tube was higher than that in the others. Liquid flow agitation by bubbles motion improved the heat transfer around the tube. Under intermittent flow condition, heat transfer coefficient flatten over the tube in comparison to that in single-phase flow. Since the void fraction around the tube was almost uniformly distributed, enhancement of the heat transfer could be obtained by bubbles motion over the entire perimeter of the tube under the condition.

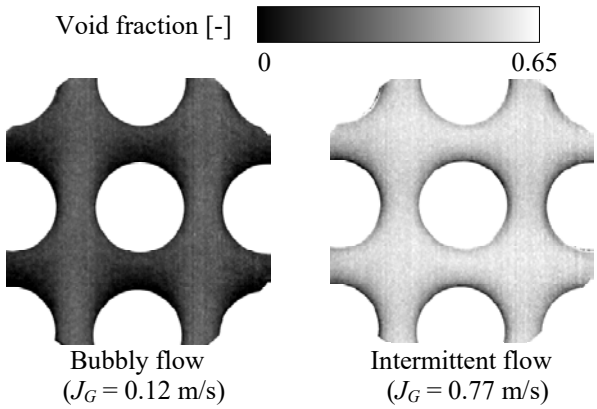

Fig. 1. Time-average two-dimensional void-fraction distributions in in-line tube bundle.

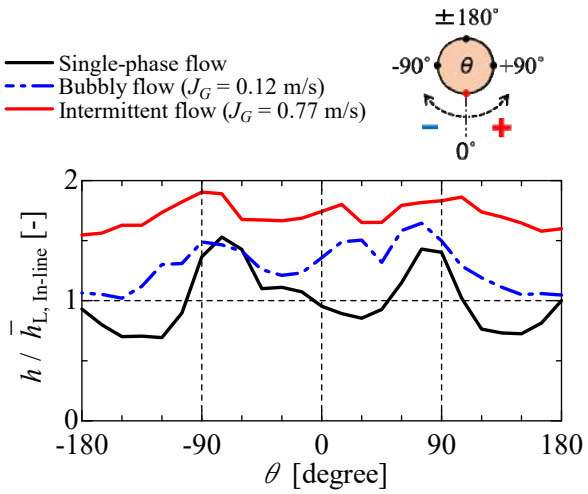

Fig. 2 Heat transfer coefficient around a tube in each flow.

REFERENCES:

[1] R. Dowlati *et al.*, AIChE Journal, **36** (1990) 765-772.
[2] D.A. McNeil *et al.*, Int. J. Multiphase Flow, **45** (2012) 53-69.
[3] G.R. Noghrehkarm *et al.*, Int. J. Multiphase Flow, **25** (1999) 857-874.

PR13-2 Estimation of Frosting Formation on the Heat Exchanger by Using X-ray Radiography

R. Matsumoto, K. Kagebayashi[1], T. Uechi[1], Y. Nagasawa[1], D. Ito[2] and Y. Saito[2]

Faculty of Engineering Science, Kansai University
[1]Graduate School of Science and Engineering, Kansai University
[2]Research Reactor Institute, Kyoto University

INTRODUCTION: Heat exchangers which are operated at below 0 °C are subjected to the frost deposition and its growth. Frost is the porous material of the crystal ice and air. The low thermal conductivity of the frost causes the low heat transfer performance. The frost density profile of the frost layer is the important property for the frost formation estimation. The frost density profiles were measured by the X-ray radiography on the cylindrical cooling surface. The three dimensional distribution of the frost deposition on the plate-fin tube heat exchanger was tried to estimate by the X-ray computed tomography at KUR B-4 radiation port.

MEASUREMENT OF FROST DENSITY PROFILE BY X-RAY RADIOGRAPHY: The photograph of the frost formation at 180 min of the frosting time on the cylindrical cooling surface at -14.0 deg.C. is shown in Fig.1(a). The frost layer was clearly shown by the X-ray beam attenuation in the radiography image, Fig.1(b). The X-ray generator was operated at 80kV and 5mA.

To estimate the frost density profile quantitatively, the mass attenuation coefficients of the water and the ice were measured by the calibration test. The gradient of Fig.2 corresponds to the mass attenuation coefficient. Experimental results of the water was close agreement with the reference value. The mass attenuation coefficient of the ice shows higher value than that of the water. The mass attenuation coefficient for the frost density estimation was used that of the ice.

Abel inversion was applied to the X-ray image to reconstruct the frost density profiles under the circularly symmetric frost formation condition around the cylindrical surface [1]. The frost density profile is shown in Fig. 3 at the 16 mm from the reading edge of the cylindrical cooling surface. The experimental result is almost the same density profiles with the previous researches [1], [2]. High frost density is appeared near the cooling surface. Frost density increased with the frosting time. At 180 min after frosting, the density profile shows a relative maximum at a distance about 3 mm from the cooling surface.

3-D FROST DENSITY PROFILE ON THE HEAT EXCHANGER ESTIMATED BY X-RAY COMPUTED TOMOGRAPHY: The three dimensional distribution of the frost deposition on the plate-fin tube heat exchanger was tried to estimate by the X-ray CT. Fig.4 shows a schematic of the experimental setup with rotating stage. On the present step of this research, the 3-D frost density distribution is not success due to the less attenuation by the frost layer on the X-ray CT. In the next stage, the X-ray imaging conditions are modified.

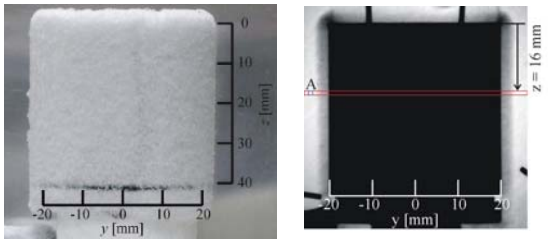

(a) Digital camera image (b) X-ray radiography image
Fig.1 Frost layer on the cylindrical cooling surface at 180 min of frosting time.

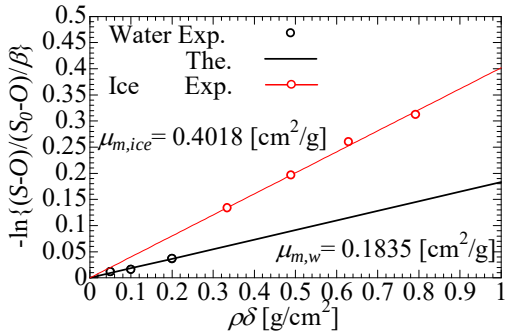

Fig.2 Mass attenuation coefficient of water and ice.

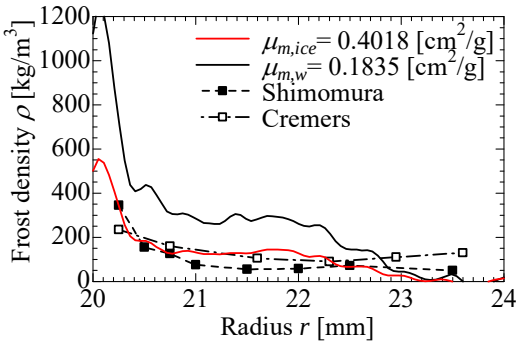

Fig. 3 Distributions of frost density profiles.

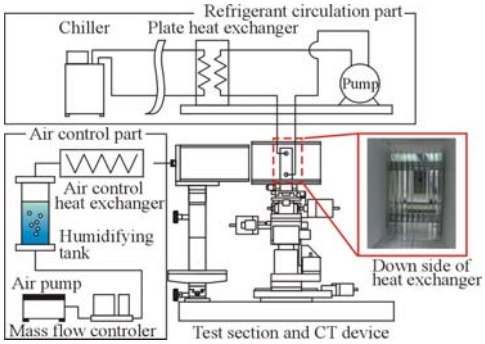

Fig. 4 Experimental setup for estimation the 3-D frost density distributions.

REFERENCES:

[1] C. J. Cremers, et al., Advances in Cryogenic Eng., **23** (1978), 371-375.
[2] N. Shimomura, et al., Trans. of the JSRAE, **19**(3) (2002), 245-254.